PHOTON BEAM POSITION MONITOR AT SIAM PHOTON SOURCE

P. Sudmuang, S. Chaichual, N. Suradet, S. Boonsuya, N. Sumano, S. Krainara, H. Nakajima, S. Rugmai, P. Klysubun
Synchrotron Light Research Institute, 111 University Avenue, Muang District,
Nakhon Ratchasima 30000, Thailand

Abstract

Photon beam position monitors (PBPM) have been designed and installed in the beamline front-ends at Siam Photon Source (SPS). Up till now, these blade-type PBPMs have been successfully installed at three bending magnet and an insertion device (planar undulator) beamlines. Their performance has been tested and compared with that of the electron beam position monitor. The achieved resolution is found to be better than 3 μm. The obtained PBPM data proved to be extremely invaluable in the investigation of the sources of the observed beam positional fluctuation, and for compensation of the orbit perturbation caused by undulator gap change. In this paper, the details of the calibration procedure will be presented. Various factors affecting reading of the signal such as undulator gap change effect, choice of bias voltage, and temperature variation have been investigated and the results will be discussed herewith.

INTRODUCTION

The Siam Photon Source (SPS) is a dedicated 1.2 GeV synchrotron light source in Thailand [1]. Currently, there are seven photon beamlines in operation, with three more under commissioning. In addition, there are three new photon beamlines under construction. As the number of experiments increases, coupled with the fact that more complicate experiments are being carried out, there is more demand from the users for higher quality beam, especially with regards to the beam positional stability aspect. In recent years the machine group has focused its effort to achieve this goal [2]. To investigate the sources of the beam position fluctuation and observe the subsequent improvement quantitatively, Photon Beam Position Monitors (PBPMs) have been developed and installed. Several types of PBPMs have been developed at synchrotron facilities around the world [3-4]. For SPS, the 4-blade type PBPM is chosen.

In this paper, the PBPM structure together with the criteria for blade spacing determination are presented, followed by the details of the calibration procedure, and various factors affecting the sensitivity and linearity threshold of the PBPM. In addition, the experiments for testing PBPM performance are described.

PBPM DESIGN

PBPM Structure

Figure 1(a) shows the design of the 4-blade type PBPM structure. The blades are triangular and were made of 0.2 mm-thick tungsten. The upper pair was affixed to a water-cooled copper block at the front facing the beam, while the lower pair was placed at the rear end. The blades were slotted in sapphire plates for electrical insulation and thermal conduction. A biased photoelectron collector was installed on each side of the copper block to remove the scattered photoelectrons. The PBPM block is attached to an XY translation stage for alignment and calibration processes. The schematic layout of the whole PBPM setup is shown in Figure 1(b). Generated photocurrent is measured by a picoammeter (Keithley 6485). To investigate thermal effect on the measured photocurrent, a thermocouple was installed on the copper block.

(a)   (b)
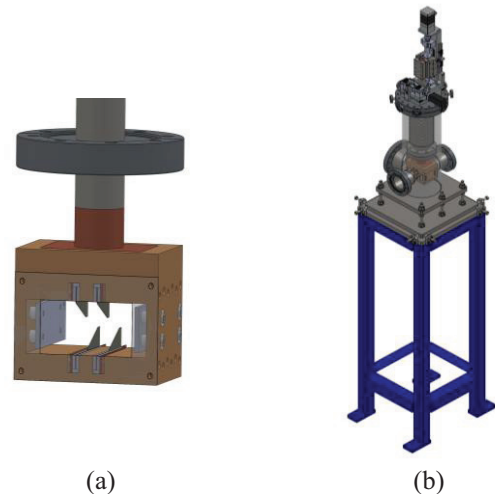
Figure 1: 3D drawings of (a) the 4-blade type PBPM block, and (b) the whole PBPM setup.

Determination of the Blade Spacing

The spacing between the blades (G_x, G_y), as shown in Figure 2, are determined by the photon beam power densities at the location of the PBPM. In order to optimize the sensitivity and linearity range, the spacing should be two times the Gaussian width, i.e. $G = 2\sigma$, except for G_x of the bending magnet PBPM, which is specified by the horizontal opening angle of a particular photon beamline. To avoid cross-talk among the blades, the upper and lower blades were shifted by 2 mm (D) apart.
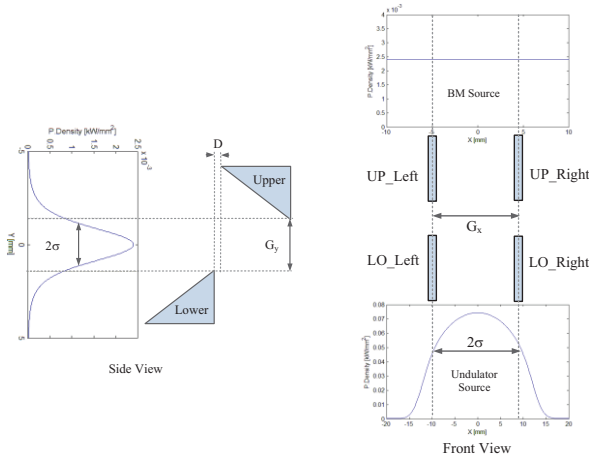
Figure 2: Blade spacing geometry.

PBPM CALIBRATION

Photon Beam Position Calculation

The PBPM calibration was performed by scanning the BPM block across the photon beam with the translation stage. Measured photocurrent on the blades are used to determined the photon beam position (x,y) in the linear region as

$$x, y = \frac{P}{S} \qquad (1)$$

where P is the beam position signal and S is the sensitivity.

The beam position signal was commonly calculated via the difference-over-sum formulae, i.e.

$$P_{x_{\Delta/\Sigma}} = \frac{\Sigma(I_R) - \Sigma(I_L)}{\Sigma(I_R) + \Sigma(I_L)} \qquad (2)$$

$$P_{y_{\Delta/\Sigma}} = \frac{\Sigma(I_{UP}) - \Sigma(I_{DN})}{\Sigma(I_{UP}) + \Sigma(I_{DN})} \qquad (3)$$

The photon beam signal can also be calculated with the log-ratio method as

$$P_{x_{Log}} = \log\left(\frac{\Sigma(I_R)}{\Sigma(I_L)}\right) \qquad (4)$$

$$P_{y_{Log}} = \log\left(\frac{\Sigma(I_{UP})}{\Sigma(I_{DN})}\right) \qquad (5)$$

where P_x and P_y is the photon beam signal in horizontal and vertical directions, respectively. I_{UP} and I_{DN} are the current from the upper and lower blades, and I_R and I_L are the current from the right and left blades, in that order.

The sensitivity was obtained from the slope of the linear fit of the measured beam position signal with respect to the PBPM block translation, displayed in Figure 3. By comparing the photon beam signals $P_{\Delta/\Sigma}$ and P_{Log}, it was found that the linear region of P_{Log} extends further than that of $P_{\Delta/\Sigma}$. Thus, we chose P_{Log} over $P_{\Delta/\Sigma}$ in our implementation.
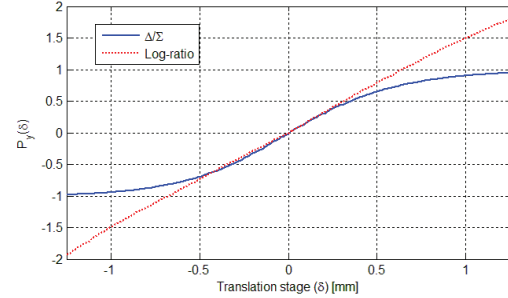
Figure 3: Measured PBPM linearity.

Bias Voltage Determination

Bias voltage is another factor influencing sensitivity and linearity of the beam position signal. Increasing the bias voltage widens the linear region while lowers the sensitivity, as depicted in Figure 4. In our case we decided that the linear region should extend at least to ± 2 mm, with acceptable sensitivity, resulting in the bias voltage of 100 V.
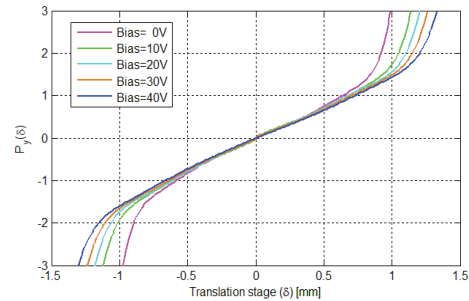
Figure 4: Measured PBPM linearity and sensitivity at different bias voltages.

Undulator Gap Change Effect

Calibration of insertion device PBPM was meticulously carried out in order to avoid or circumvent various detrimental factors such as background radiation from the bending magnet and variation of the current signal on each blade at different undulator gaps. Influence of the gap change on each individual blade is shown in Figure 5. To compute the beam position at different gaps, the sensitivity was fitted with an exponential function as

$$S = \alpha + \beta \exp(-\gamma G) \qquad (6)$$

where G is the insertion device gap, α, β, and γ are fitting parameters.
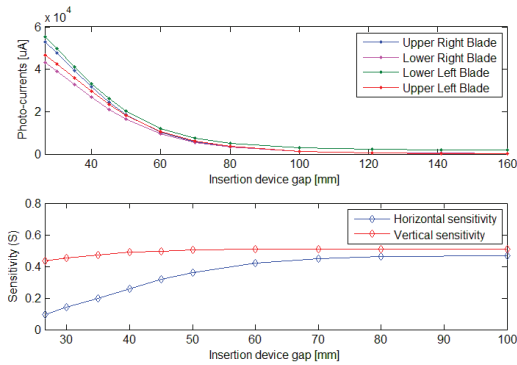
Figure 5: Variation of the (top) individual blade signals, and (bottom) sensitivity as a function of the undulator gap.

PBPM PERFORMANCE

After the PBPM was installed, we first looked at the reading while varying the setting of a vertical corrector. The measurement results are shown in Figure 6. It was found that the orbit change monitored by the PBPM is in good agreement with the electron BPM, with the PBPM giving more sensitive reading, reflecting more closely to the change of the corrector.
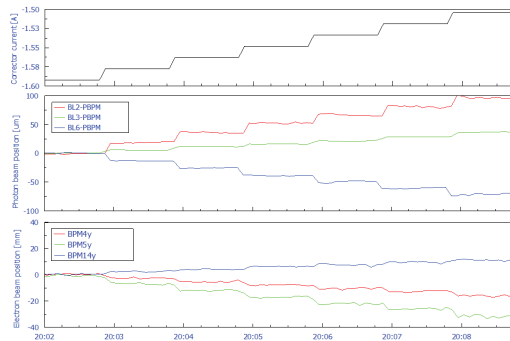
Figure 6: Measured photon and electron beam position as a function of the corrector magnet current.

Figure7 shows the vertical beam position obtained from bending magnet and insertion device PBPM together with the temperature variation measured on the copper block inside the vacuum chamber. Temperature variation of the copper block was restricted to within $\pm 0.25\ ^{O}$C by the cooling water, and thus does not affect the photon beam position reading. By measuring the short-term beam position, the resolution was observed to be better than 3 μm.

The undulator look-up table was created by incorporating the photon beam position reading obtained from the PBPM. In doing so, significant improvement over the normal case, where only electron BPM is taken into account, has been achieved (Figure 8). Since the installation the more accurate PBPM reading enable the machine group to pinpoint more easily the various sources perturbing the beam such as power supply ripple,

air temperature fluctuation, vacuum pressure problem, etc.
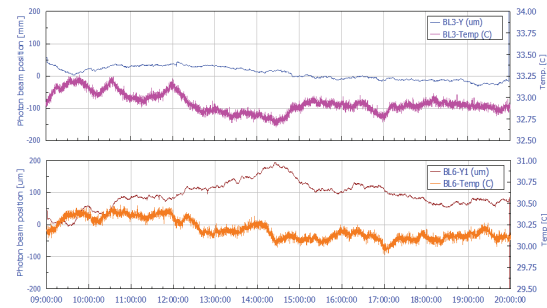
Figure 7: Measured photon beam position and temperature variation during user beam operation.
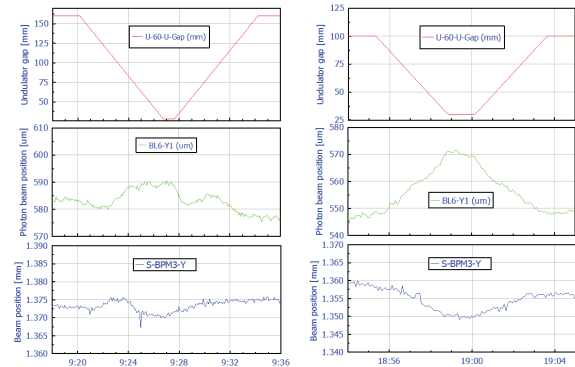
Figure 8: Compensation of the orbit perturbation caused by undulator gap change with (left) and without (right) incorporating the PBPM reading.

CONCLUSION

The PBPM were successfully installed in the beamline front-ends at SPS. The measured photon beam position obtained by PBPM of each beamline is in good agreement with the BPM data. The PBPM has linear region that extends over ± 2 mm and has better than 3 μm resolution.

ACKNOWLEDGMENT

The authors would like to thank Changbum Kim of PLS and June Rong Chen of NSRRC for their support and advices related to PBPM design and improvement.

REFERENCES

[1] P. Klysubun et al., "Operation and improvement of the Siam Photon Source", Nuclear Instrument and Methods in Physics Research, 582 (2007), 18-21.

[2] S. Klinkhieo et al., "Commissioning results of slow orbit feedback using PID controller method for Siam photon source", IPAC'12, Louisiana, USA.

[3] H. Aoyagi et al., "Blade-type X-ray beam position monitors for SPring-8 undulator beamlines", Nuclear Instrument and Methods in Physics Research, 467 (2001), 252-255.

[4] S.F. Lin et al., "The Study of New Signal Processing Technique in Photon Beam Position Monitors", IPAC'05, Knoxville, Tennessee.